JOURNAL OF CATALYSIS 120, 46–54 (1989)

Interaction of Pyridine and Ammonia with a Sulfate-Promoted Iron Oxide Catalyst

JAE S. LEE[1] AND DOO S. PARK

Department of Chemical Engineering, Pohang Institute of Science and Technology, and Research Institute of Industrial Science and Technology, P.O. Box 125, Pohang, Korea

Received February 23, 1989; revised May 3, 1989

Interactions of sulfate–promoted iron oxide, SO_4^{2-}–Fe_2O_3, with pyridine or ammonia were investigated by means of infrared spectroscopy and temperature-programmed desorption/reaction coupled with mass spectrometry. Both molecules reacted with the sulfate group upon adsorption followed by heating to change the structure of the sulfate group and the acid properties of SO_4^{2-}–Fe_2O_3. They also promoted the decomposition of the sulfate group and its removal from the surface. These effects were more pronounced for pyridine. © 1989 Academic Press, Inc.

INTRODUCTION

Solid superacid catalysts of TiO_2, ZrO_2, and Fe_2O_3 activated with small amounts of sulfate ions SO_4^{2-} have been shown to exhibit pronounced catalytic activity for many acid-catalyzed reactions such as isomerization, dehydration, esterification, acylation, and hydrocracking (*1–6*). Superacidity of the catalysts has been proposed to originate from the formation of a surface sulfur complex with a covalent S=O double bond, and its electron induction effect which enhances the Lewis acidity of the metal cation (*6*). Structures **I** (*5*) and **II** (*7*) have been proposed for the surface sulfate species, with M denoting a metal ion.

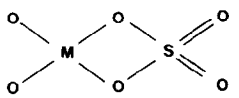

I

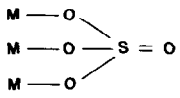

II

The sulfate deposited on the oxides is thermally stable below 770 K (*4*). However, little is known about the chemical stability of the species. It was found that under dihydrogen at 720 K, the sulfate remained on the surface although the sulfur was reduced from S^{6+} to S^{2-} (*4*). To understand the chemical stability of the species, the present study investigates the interaction of pyridine and ammonia with a sulfate–promoted iron oxide, SO_4^{2-}–Fe_2O_3. Adsorption of these basic molecules, followed by temperature-programmed desorption/reaction (TPDR) or infrared spectroscopy (IR), is commonly employed to probe the acidity of solid acid catalysts. Interaction of these molecules with the catalyst surface may also model the behavior of the catalyst during reaction.

EXPERIMENTAL

For the preparation of SO_4^{2-}–Fe_2O_3, iron hydroxide, $Fe(OH)_3$, was first prepared by treating a 3 *N* aqueous solution of $Fe(NO_3)_3$ with 3 *N* aqueous ammonia; the product was then washed and dried at 370 K for 24 h. The SO_4^{2-}–Fe_2O_3 was prepared by immersing $Fe(OH)_3$ in an aqueous solution of $(NH_4)_2SO_4$ at 350 K and then calcining the precipitate at 770 K in air or *in vacuo* for 2.5 h. To measure the content of sulfur, the sample was dissolved in a 6 *N* aqueous HCl solution. An aqueous solution of $BaCl_2$ was then added to the solution to precipitate SO_4^{2-} as $BaSO_4$, which was weighed.

[1] To whom correspondence should be addressed.

0021-9517/89 $3.00

The prepared sample was characterized by several physical methods. The powder X-ray diffraction (XRD) patterns were obtained with CuKα radiation on a Rigaku Dmax-B diffractometer. The specific surface area was measured by the N_2 BET method on a Micromeritics Accusorb 2100E for a sample calcined at 770 K. Thermogravimetric and differential thermal analysis (TGA/DTA) was performed on a Perkin–Elmer 1700 system at a heating rate of 0.33 K s^{-1} in flowing N_2 (Posco, 99.998%).

IR measurements were made with a Perkin–Elmer 1800 FT-IR spectrometer on a self-supporting disk sample. The disk was prepared by compressing the powder under 6–8 $\times$ 10^3 kg cm^{-2}. A quartz IR sample cell could be connected to a flow system for sample treatments and transferred to the spectrometer without exposing the sample to the atmosphere. Adsorption of pyridine (Wako, 98.0%) or ammonia (Matheson, anhydrous) was carried out by flowing He (Airco, 99.997%) saturated with pyridine or ammonia alone for 0.5 h onto a sample maintained at room temperature (RT). To remove moisture in pyridine, a 4-Å molecular sieve, previously treated at 670 K in He flow for 2.5 h, was added. Series of liquid N_2, 4-Å molecular sieve, and MnO/SiO_2 traps were employed to purify He. After adsorption, the sample, still maintained at RT, was flushed with He flowing at 86 μmol s^{-1} for 0.5 h to remove adsorbates in the gas phase and physisorbed on the sample. The temperature of the sample was increased at the rate of 0.17 K s^{-1} to a certain temperature, and then rapidly cooled to RT to take the IR spectra.

TPDR was performed for a 100-mg powder sample in a flow cell. The adsorption and He flush were performed in the same manner as in IR experiments. The temperature of the sample was raised at a linear rate of 0.33 K s^{-1}, in He flowing at 86 μmol s^{-1}. Desorbed products were analyzed by an online VG Micromass quadrupole mass spectrometer (MS).

RESULTS

Characteristics of the Sample

After calcination at 770 K for 2.5 h, the SO_4^{2-}–Fe_2O_3 contained 3.2 wt% sulfur as SO_3 as determined by precipitated $BaSO_4$. The BET surface areas of Fe_2O_3 and SO_4^{2-}–Fe_2O_3 were 19 and 30 m^2 g^{-1}, respectively. The Fe_2O_3 was obtained by calcining $Fe(OH)_3$ at 770 K. Both Fe_2O_3 and SO_4^{2-}–Fe_2O_3 showed identical XRD patterns of hematite (α-Fe_2O_3). No bulk iron sulfate phase was detected. The TGA/DTA curves in Fig. 1 indicate that the SO_4^{2-}–Fe_2O_3 sample is thermally stable up to 770 K. The decrease in weight in the TGA curve starts to be seen from ca. 820 K. A corresponding DTA response is an endotherm with a peak around 920 K. There are only negligible variations in TGA/DTA curves for Fe_2O_3.

Infrared spectra of the sample evacuated at increasing temperatures are shown in Fig. 2. The spectra for the sample evacuated at low temperatures indicate the presence of water, showing bands near 3600 and 1610 cm^{-1}. Bands between 900 and 1300 cm^{-1} are due to SO_4^{2-}. Evacuation at 770 K removes water bands completely, and a band at 1240 cm^{-1} moves to 1379 cm^{-1}. This sharp band at 1379 cm^{-1} due to the asymmetric vibration of the S=O bond has been used as a fingerprint of a well-prepared SO_4^{2-}–Fe_2O_3 sample with superacidity (5). All these characteristics of our sample agree with those reported previously for

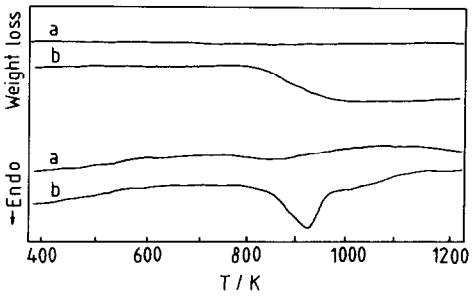

Fig. 1. TGA/DTA curves of Fe_2O_3 (a) and SO_4^{2-}–Fe_2O_3 (b).

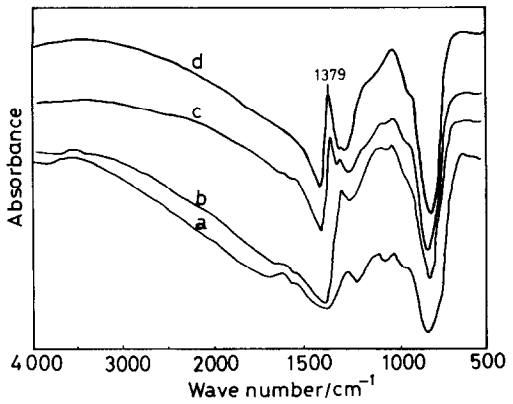

Fig. 2. IR spectra of SO_4^{2-}–Fe_2O_3 dried at 370 K in air (a), and evacuated at 370 K (b), 570 K (c), and 770 K (d).

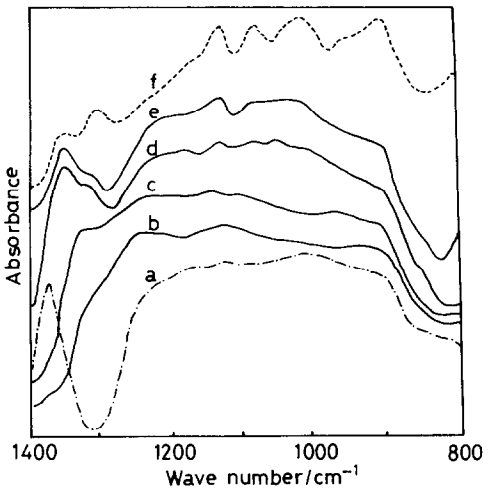

Fig. 3. Infrared spectra (800–1400 cm^{-1}) of SO_4^{2-}–Fe_2O_3 before and after adsorption of pyridine. The fresh sample was treated at 760 K for 2 h in He flowing at 86 μ mol s^{-1} (a). After adsorption of pyridine at RT, the sample was treated in He flow at RT (b), 420 K (c), 620 K (d), 670 K (e), and 720 K (f).

many sulfate-promoted metal oxide catalysts showing superacidity (*3–7*).

Infrared Spectrum of Adsorbed Pyridine

The IR spectrum of SO_4^{2-}–Fe_2O_3 treated in He at 760 K for 2 h (Fig. 3a) shows the characteristic S=O band at 1382 cm^{-1} together with broad bands in the range 900–1250 cm^{-1}. The spectrum is almost the same as that in Fig. 2 for the sample evacuated at 770 K. When pyridine is adsorbed, the sharp band at 1382 cm^{-1} disappears and new band appears near 1315 cm^{-1} (Fig. 3b). As the temperature of the pyridine-adsorbed sample is increased, this new band shifts to higher wavenumbers, and another new band appears near 1310 cm^{-1} above 620 K (Fig. 3d). At 720 K, two bands grow to become comparable in intensity and bands at 900–1140 cm^{-1} become sharper (Fig. 3f). The band at highest wavenumber is located at 1360 cm^{-1}, about 20 cm^{-1} lower than for the fresh sample before adsorption of pyridine.

The IR spectra of adsorbed pyridine in the range 1400–1700 cm^{-1} (Fig. 4) represent acid properties of the solid (*8*). The spectrum after He flush at RT (Fig. 4a) exhibits sharp bands at 1450 and 1610 cm^{-1} due to Lewis acid sites and a broad band at 1540 cm^{-1} due to Brønsted acid sites. Both Lewis and Brønsted acid sites give rise to the band at 1490 cm. A shoulder around 1440 cm^{-1} is due to hydrogen-bonded pyridine. As the temperature of He treatment is raised, the band at 1450 cm^{-1} shifts toward 2–3 cm^{-1} higher wavenumbers (Fig. 4b–d). Above 520 K, new bands appear at 1472

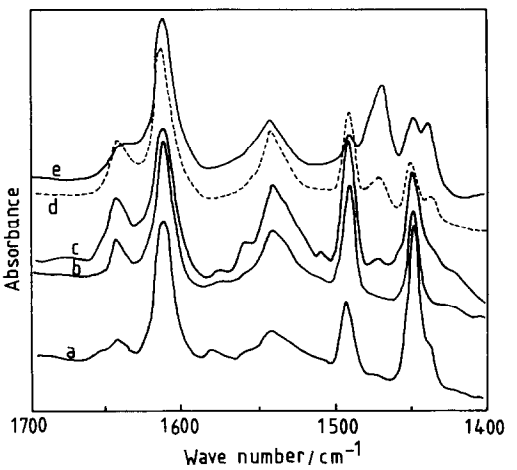

Fig. 4. Infrared spectra (1400–1700 cm^{-1}) of the same sample as in Fig. 3. The sample was treated in He flow at RT (a), 420 K (b), 520 K (c), 620 K (d), and 670 K (e).

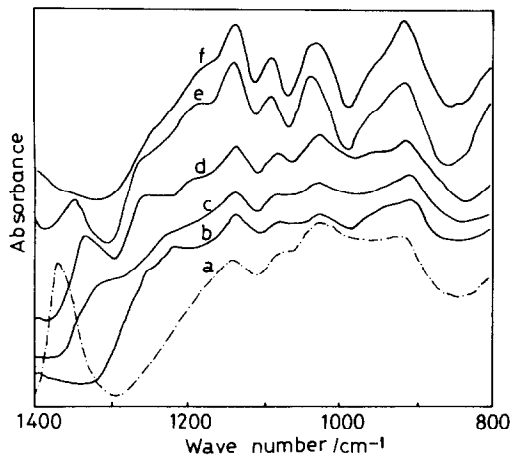

Fig. 5. Infrared spectra (800–1400 cm^{-1}) of an oxidized sample before and after adsorption of pyridine. The sample was treated at 760 K for 1 h in O_2 flowing at 25 μmol s^{-1} (a). After adsorption of pyridine at RT, the sample was treated in He flow at RT (b), 420 K (c), 620 K (d), 670 K (e), and 720 K (f).

and 1437 cm^{-1}, and become even sharper than the original band located near 1450 cm^{-1}. The sample treated at 760 K (not shown) loses most of the IR features.

Since the sample treated in He at 760 K after pyridine adsorption did not recover the original S=O band near 1380 cm^{-1}, the sample was treated at 760 K for 1 h in O_2 flowing at 25 μmol s^{-1} to determine whether the treatment would recover the original sulfate structure. As shown in Fig. 5a, the oxidized sample exhibits a strong band at 1368 cm^{-1}. This is 14 cm^{-1} lower than the 1382 cm^{-1} for the fresh sample. Adsorption of pyridine and treatments in He were performed on this sample in the same manner as for the fresh sample, and IR spectra were taken. When pyridine is adsorbed, the band at 1368 cm^{-1} shifts to 1240 cm^{-1} (Fig. 5b). The band shifts to higher wavenumbers as the temperature increases (Fig. 5c–e), but disappears at 720 K (Fig. 5f). Little change is observed for bands at 900–1140 cm^{-1}. It should be noted that unlike the fresh sample, the oxidized sample shows a single band near 1350 cm^{-1}.

The IR spectra of adsorbed pyridine in Fig. 6 exhibit only two dominant bands, at 1610 and 1450 cm^{-1}. Especially noteworthy is that the band at 1490 cm^{-1} denoting the presence of Lewis and/or Brønsted acid sites has a vanishingly small intensity. The spectra could be assigned as pyridine hydrogen-bonded to an –OH group (*8*). Similar spectra have been reported for hydrogen-bonded pyridine adsorbed on silica (*9*). Spectra in the range 2600–4000 cm^{-1} showed NH, CH, and OH stretching bands. As the temperature of He treatment is increased, two bands at 1472 and 1437 cm^{-1} appear again as for the fresh sample.

After the He treatment at 720 K, O_2 treatment followed by pyridine adsorption was repeated. This reoxidized sample showed IR spectra very similar to those in Figs. 5 and 6 for the sample oxidized for the first time.

Infrared Spectrum of Adsorbed Ammonia

Ammonia was adsorbed on fresh SO_4^{2-}–Fe_2O_3, showing the IR spectrum in Fig. 7a. As before, the ammonia-adsorbed sample was treated at increasing temperatures in flowing He, and IR spectra were taken. In Fig. 7, adsorption of ammonia at RT moves the S=O peak at 1382 cm^{-1} to 1300 cm^{-1}. Unlike the case of pyridine, however, this

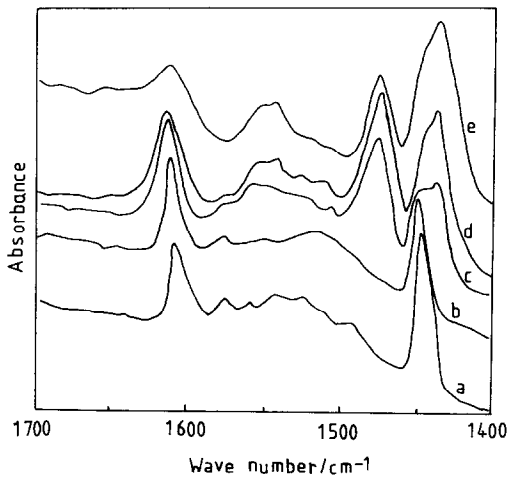

Fig. 6. Infrared spectra (1400–1700 cm^{-1}) of the same sample as in Fig. 5. The sample was treated in He flow at RT (a), 420 K (b), 520 K (c), 620 K (d), and 670 K (e).

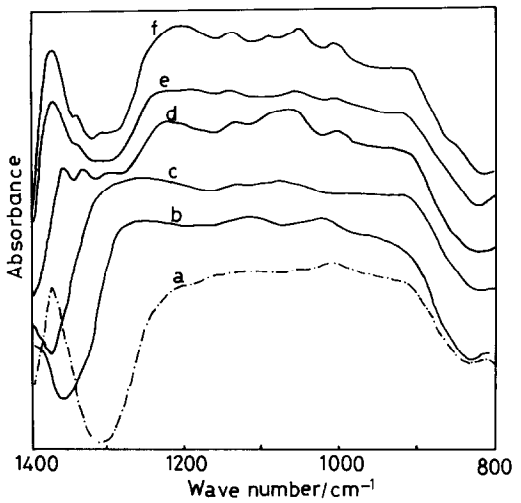

Fig. 7. Infrared spectra (800–1400 cm^{-1}) of SO_4^{2-}–Fe_2O_3 before and after adsorption of ammonia. The fresh sample was treated at 760 K for 2 h in He flowing at 86 μmol s^{-1} (a). After adsorption of ammonia at RT, the sample was treated at RT (b), 420 K (c), 620 K (d), 670 K (e), and 720 K (f).

peak shifts back almost to the original position of 1380 cm^{-1} as the temperature is increased. The presence of a small shoulder near 1340 cm^{-1} in Fig. 7f is the only noticeable difference from the IR spectrum of the fresh sample.

The IR spectra of adsorbed ammonia in Fig. 8 show bands at 1610 and 1450 cm^{-1}

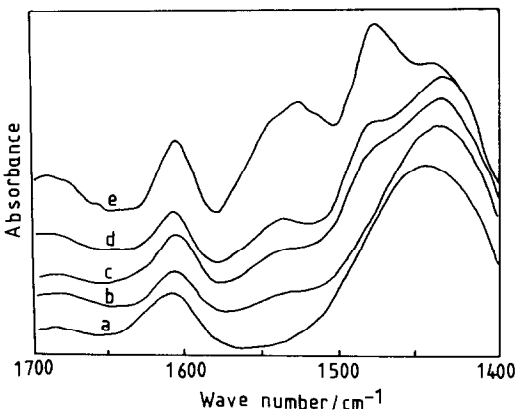

Fig. 8. Infrared spectra (1400–1700 cm^{-1}) of the same sample as in Fig. 7. The sample was treated in He flow at RT (a), 420 K (b), 520 K (c), 620 K (d), and 670 K (e).

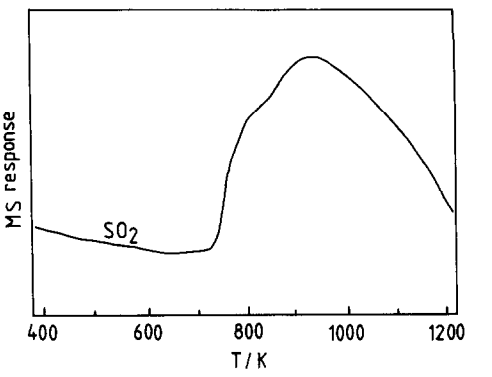

Fig. 9. TPDR curve for SO_4^{2-}–Fe_2O_3.

representing, respectively, the presence of Lewis and Brønsted acid sites (*8*). As the temperature is increased, new peaks appear at 1490 and 1530 cm^{-1}.

Temperature-Programmed Desorption/Reaction

When SO_4^{2-}–Fe_2O_3 was heated in a He flow and the gas phase was analyzed by MS, the TPDR spectrum in Fig. 9 was obtained. The spectrum indicates that SO_4^{2-}–Fe_2O_3 starts to decompose at 750 K to produce gaseous SO_2, and that sulfate is mostly removed from the surface below 1100 K. The presence of a shoulder at the low-temperature side suggests that the thermal stability of SO_4^{2-} is not uniform. From TGA/DTA measurement, Jin *et al.* (*4*) suggested that SO_4^{2-} decomposed to yield gaseous SO_3. In our MS analysis, however, *m/e* 80 corresponding to molecular SO_3 was absent. It should be noted that the decomposition temperature of SO_4^{2-} found by TPDR agrees well with that observed by TGA/DTA in Fig. 1.

The sample with preadsorbed pyridine showed a very complicated TPDR spectrum as shown in Fig. 10. In addition to SO_2 (*m/e* 64 or 48), desorbed pyridine (*m/e* 79 or 52), N_2 (*m/e* 28), and CO_2 (*m/e* 44) were detected in the gas phase. Water (*m/e* 18) was also detected, but in an insignificant amount. The most significant change is that preadsorption of pyridine appears to lower

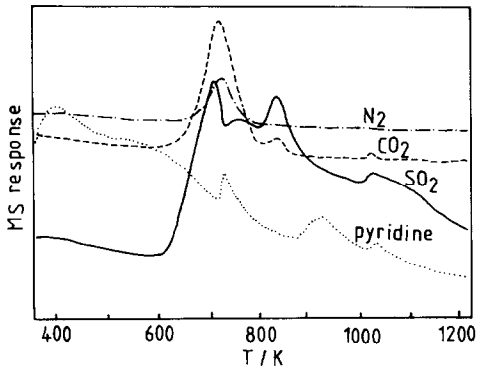

Fig. 10. TPDR curve for SO_4^{2-}–Fe_2O_3 with adsorbed pyridine.

the decomposition temperature of SO_4^{2-}. Formation of SO_2 starts from 620 K and its TPDR spectrum becomes complicated. Pyridine desorbs in many stages over a broad temperature range. Even at 1000 K, a peak is found in its TPDR spectrum. The presence of CO_2 and N_2 with peaks at the same peak temperature of SO_2 formation indicates that a part of pyridine decomposes by a reaction with SO_4^{2-}. The source of oxygen in CO_2 must be SO_4^{2-}–Fe_2O_3. Furthermore, in a blank experiment, pyridine was found to thermally decompose only above 1100 K in the empty TPDR cell without SO_4^{2-}–Fe_2O_3.

As shown in Fig. 11, the destabilization of SO_4^{2-} by ammonia adsorption is not as great as that for pyridine. However, ammonia changes the shape of the TPDR spectrum for SO_2 significantly. The formation of N_2 also suggests that part of the ammonia decomposes as the result of a reaction with SO_4^{2-}–Fe_2O_3. As before, a blank experiment indicated that thermal decomposition of ammonia was significantly only above 870 K.

DISCUSSION

Interactions between Pyridine and SO_4^{2-}–Fe_2O_3

In catalysis by sulfate-promoted metal oxides or in characterization of these catalysts by adsorption of probe molecules, the sulfate group has been assumed to induce the removal of electrons from the metal ion, to enhance the Lewis acidity of the metal ion site, and not to interact directly with reactants or probe molecules (*6*). The results of the present study demonstrate that this spectator role of the sulfate group is true only below the temperature at which the reactants begin to react with sulfate and remove it from the catalyst surface.

It has been known that SO_4^{2-}–Fe_2O_3 contains mostly Lewis acid sites. Infrared spectra reported by Jin *et al.* (*6*) showed bands only for pyridine adsorbed on Lewis acid sites of SO_4^{2-}–Fe_2O_3. The band at 1540 cm^{-1} in Fig. 4 appears to be due to Brønsted sites that are generated by moisture inadvertently introduced into the system, as also observed by Saur *et al.* (*7*). It should be noted that the spectra of Jin *et al.* were recorded *in vacuo,* whereas those in the present study were obtained in flowing He. Despite all the precautions we took to dry the gas stream and pyridine, a considerable amount of water may have been introduced into the system, as indicated by the presence of the 1540 cm^{-1} band. Indeed, the intensity of this band varied significantly depending on the flow rate of He and other experimental conditions. However, water is not known to affect the stability of SO_4^{2-}–Fe_2O_3 (*3*). Because of the adsorption of pyridine on the Fe site and the electron

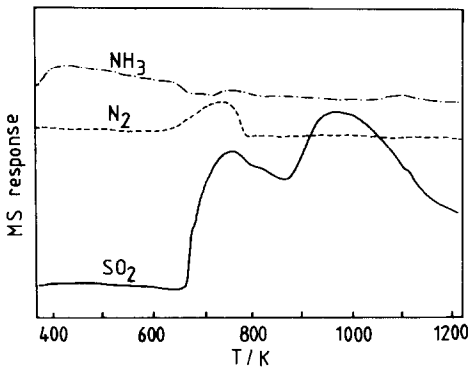

Fig. 11. TPDR curve for SO_4^{2-}–Fe_2O_3 with adsorbed ammonia.

shift from this basic molecule, the sulfate ion loses its double bond character; thus, the characteristic IR band at 1382 cm^{-1} shifts to 1315 cm^{-1} (Fig. 3a,b). When the sample is heated in a He flow, not all of the pyridine desorbs molecularly. Some of the pyridine reacts with the sulfate group to change its structure or to destroy and remove it from the surface. The decomposition products include SO_2, CO_2, and N_2 as shown in Fig. 10. The presence of CO_2 proves that a reaction has occurred between pyridine and sulfate, the respective sources of carbon and oxygen.

A change in the structure of sulfate is indicated in the IR spectra in Figs. 3 and 4. Heating up to 720 K did not lead to recovery of the original S=O band. Instead, above 620 K, two new bands appear which are finally located at 1360 and 1310 cm^{-1} (Fig. 3f) at 720 K. In Fig. 4, new bands also appear at 1472 and 1437 cm^{-1} at 520 K, outgrowing the original bands due to Lewis acid sites. The TPDR spectra shown in Fig. 10 indicate that less than half of the sulfur present in a fresh sample is removed by pyridine adsorption and TPDR up to 770 K, the highest temperature in the IR experiments. Dioxygen treatment recovers the S=O spectrum at 1368 cm^{-1} (Fig. 5a), but the IR spectrum of pyridine adsorbed on this oxidized sample (Fig. 6a) differs completely from that on a fresh sample. The spectrum in Fig. 6a could be interpreted as pyridine hydrogen-bonded to an –OH group (*8*). The IR spectrum of the oxidized sample upon subsequent heating, behaves like that of the fresh sample, except that only one band remains at 1350 cm^{-1}. It was noted that this band is related to the band at 1472 and 1436 cm^{-1} due to pyridine: they appear and disappear together. They may arise from the same species. The species appears to contain reduced sulfur since it is oxidized back to the original S(VI) by O_2 treatment. What then is the surface species that gives rise to these bands?

Many studies have reported the positions of IR bands for pyridine adsorbed on Lewis acid sites. Recent examples include Fe/SiO_2 (*10*), (Ti, V, or Mo)/SiO_2 (*11*), WO_3/Al_2O_3 (*12*), heteropoly acids (*13*), TiO_2 (*14*), ion-exchanged mordenite (*15*), metal ions/SiO_2 (*16*), TiO_2/ZnO (*17*), and ZrO_2 (*18*). All of these examples reported the band positions between 1447 and 1460 cm^{-1} for 19b mode and between 1488 and 1503 cm^{-1} for 19a mode (*8*). The modes were assigned by Kline and Turkevich (*19*). A rather high wavenumber of 1462 cm^{-1} for 19b was reported for pyridine adsorbed on dealuminated mordenite when evacuated above 670 K (*20*). The origin of this strong Lewis acid site was attributed to the polarization by a "hydroxy nest" formed when pyridine adsorbed at neighboring Brønsted sites was desorbed by the high-temperature evacuation. Hence, the bands at 1472 and 1437 cm^{-1} are not likely to be due to pyridine adsorbed on Lewis acid sites. Table 1 shows the locations of the S=O group in various environments (*21*). The most probable species near 1350 cm^{-1} is $-SO_2N-$. Based on this information, a species with structure **III** could be proposed.

TABLE 1

IR Bands of Various S=O Groups

S=O group	IR band position (cm^{-1})
–O–SO–O–	1205
$-SO_2-OH$	1160, 1070
R–SO–R	1020
$R-SO_2-R$	1325, 1135
$-O-SO_2-O-$	1400, 1190
$-SO_2N-$, $-SO_2-O-R-$	1340, 1175

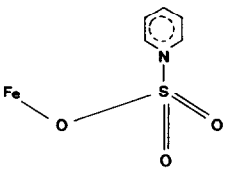

III

Hence, the IR bands at 1472 and 1437 cm^{-1} could be assigned to pyridine coordinated to sulfur. Species **III**, upon O_2 treatment, is converted to a species with a structure similar but not identical to that of the original species, **I** or **II**, because the S=O band occurs at 1468 cm^{-1} (Fig. 5a) and only pyridine hydrogen-bonded to an –OH group is detected by IR (Fig. 6). Possibly, the –OH group is bonded to Fe, thus blocking direct coordination of pyridine.

Interactions between Ammonia and SO_4^{2-}–Fe_2O_3

Ammonia appears to behave in a less complicated manner than pyridine in the interaction with SO_4^{2-}–Fe_2O_3. First, destabilization of the sulfate group is not severe as seen in Figs. 9 and 11. However, decomposition of ammonia could be noted from the presence of N_2. Second, Fig. 7 shows that the original S=O IR spectrum of the fresh sample is almost recovered upon heating above 670 K, except for a small shoulder at 1340 cm^{-1}. Figure 8 also shows new bands at 1470 cm^{-1} and 1530 cm^{-1}, which appear when the ammonia-adsorbed sample is heated above 520 K. This could be assigned to amine, $-NH_2$ (*21*). Thus, the species **IV** can be proposed.

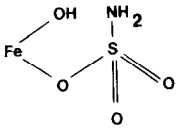

IV

There were bands at 3500 and 3600 cm^{-1} which are believed to be due to –OH and $-NH_2$, respectively. The formation of this amine species may be responsible for the early decomposition of ammonia around 670 K in TPR. In general, the interaction of SO_4^{2-}–Fe_2O_3 with ammonia resembles that with pyridine in nature, but takes place with much less severity. This appears to be due to the higher reactivity of pyridine with the sulfate group.

CONCLUSION

Sulfate-promoted iron oxide is *thermally* stable up to 770 K, but is much less stable *chemically*. Pyridine or ammonia preadsorbed on the sample reacts with the sulfate group upon heating and causes (i) a change in the structure of the surface sulfate group and the acid properties of the sample, and (ii) decomposition of the sulfate group and its removal from the surface at temperatures lower than those for thermal decomposition. These effects are much more pronounced for pyridine. This reactivity of the sulfate group must be taken into consideration when pyridine or ammonia is employed as a probe molecule of surface acidity. The results also suggest that interactions between the sulfate group and any reactants are possible when the sulfate-promoted metal oxides are used as acid catalysts.

ACKNOWLEDGMENT

This work has been partly supported by the Korean Science and Engineering Foundation (K72320).

REFERENCES

1. Hino, H., and Arata, K., *Chem. Lett.*, 477 (1979).
2. Tanabe, K., Kayo, A., and Yamaguchi, T., *J. Chem. Soc. Chem. Commun.*, 602 (1981).
3. Kayo, A., Yamaguchi, T., and Tanabe, K., *J. Catal.* **83,** 99 (1983).
4. Jin, T., Machida, M., Yamaguchi, T., and Tanabe, K., *Inorg. Chem.* **23,** 4396 (1984).
5. Yamaguchi, T., Jin, T., and Tanabe, K., *J. Phys. Chem.* **90,** 3148 (1986).
6. Jin, T., Yamaguchi, T., and Tanabe, K., *J. Phys. Chem.* **90,** 4794 (1986).
7. Saur, O., Bensitel, M., Saad, A. B. M., Lavalley, J. C., Tripp, C. P., and Morrow, B. A., *J. Catal.* **99,** 104 (1986).
8. Tanabe, K., "*Solid Acids and Bases: Their Catalytic Properties*," p. 27. Academic Press, New York, 1970.
9. Little, L. H., "*Infrared Spectra of Adsorbed Species*," p. 196. Academic Press, New York, 1966.
10. Connel, G., and Dumesic, J. A., *J. Catal.* **101,** 103 (1986).
11. Kataoka, T., and Dumesic, J. A., *J. Catal.* **112,** 66 (1988).
12. Soled, S. L., McVicker, G. B., Murrell, L. L. Sherman, L. G., Dispenziere, Jr., N. C., Hsu, S. L., and Waldman, D., *J. Catal.* **111,** 286 (1988).

13. Kim, J.-S., Kim, J.-M., Seo, G., Park, N.-C., and Niiyama, H., *Appl. Catal.* **37,** 45 (1988).
14. Buska, G., Saussey, H., Saur, O., Lavalley, J. C., and Lorenzelli, V., *Appl. Catal.* **14,** 245 (1985).
15. Kojima, M., Rautenbach, M. W., and O'Connor, C. T., *J. Catal.* **112,** 505 (1988).
16. Connel, G., and Dumesic, J. A., *J. Catal.* **105,** 285 (1987).
17. Lercher, J. A., Vinek, H., and Noller, H., *Appl. Catal.* **12,** 293 (1984).
18. Nakano, Y., Lizuka, T., Hattori, H., and Tanabe, K., *J. Catal.* **57,** 1 (1979).
19. Kline, C. H., Jr., and Turkevich, K., *J. Chem. Phys.* **12,** 300 (1944).
20. Ghosh, A. K., and Curthoys, G., *J. Chem. Soc. Faraday Trans 1* **70,** 805 (1983).
21. Pouchert, C. J., "*The Aldrich Library of Infrared Spectra,*" 3rd ed. Aldrich Chemical Co., Milwaukee, Wisconsin, 1981.